VIRTUAL SCREENING OF POTENTIAL THERAPEUTIC INHIBITORS AGAINST SARS-CoV-2 MAIN PROTEASE

Name of the supervisor- Dr. Raj Kumar

Name of the student- Vaibhav Gangta

Enrollment No.-171506

JUNE 2021

DEPARTMENT OF BIOTECHNOLOGY AND BIOINFORMATICS,
JAYPEE UNIVERSITY OF INFORMATION TECHNOLOGY,
WAKNAGHAT, SOLAN 173234, HIMACHAL PARDESH, INDIA

ACKNOWLEDGEMENT

I take the opportunity to express profound sense of gratitude to **Prof. Dr. Sudhir Kumar, Professor and Head of the Department of Biotechnology and Bioinformatics, Jaypee University of Information Technology, Waknaghat, India,** without whom, this Project would not have been possible.

I am extremely thankful to **Dr Raj Kumar, Assistant Professor of the Department of Biotechnology and Bioinformatics, Jaypee University of Information Technology, Waknaghat, India** who helped me in my queries, guided me in doing a lot of research and I came to know about so many new things I am really thankful to him.

Lastly, I would like to thank all my friends, colleagues and my parents for their blessing and moral support that always encourages me to overcome all the difficulties in my life with a positive attitude.

DECLARATION BY THE STUDENT

I hereby declare that the work presented in the B.Tech project report entitled, "**Virtual Screening of potential therapeutic inhibitors against SARS-COV-2 Main Protease"** in fulfilment of the requirement for the Final Year Project submitted at the department of **Biotechnology and Bioinformatics, JUIT Waknaghat** is an authentic record of my own work carried out under the supervision of **Dr. Raj Kumar**. I have not submitted this work elsewhere for any other degree or diploma.

(Signature of the Student)

Vaibhav Gangta (171506)

Department of Biotechnology and Bioinformatics,

Jaypee University of Information Technology,

Waknaghat, India

Date: 15/05/2021

CERTIFICATE

This is to certify that the project entitled "Virtual Screening of potential therapeutic inhibitors against SARS-COV-2 Main Protease", submitted by Vaibhav Gangta is in its partial fulfillment for the award of degree of Bachelor of Technology in Bioinformatics to Jaypee University of Information Technology Waknaghat, Solan, (H.P), India is an authentic record of candidate's own work carried out by them under my supervision.

This work has not been submitted partially or fully to any other university or institute in order to achieve any award or other degree.

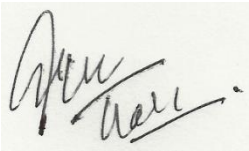

Dr. Raj Kumar

Assistant Professor,

Department of Biotechnology and Bioinformatics.

Jaypee University of Information Technology,

Waknaghat, (173234), India

TABLE OF CONTENTS

LIST OF FIGURES

LIST OF TABLES

1. ABSTRACT

Severe Acute Respiratory Syndrome Coronavirus 2 (SARS-CoV-2) is a type of betoacornavirus that targets the respiratory organs of host organism. It is responsible for causing the COVID-19 pandemic. The coronavirus disease (COVID-19) first reported in the year 2019 originating from the Wuhan city of China. Due to its high transmission rates, the entire world has been affected by the damage it has caused, whether financially or in terms of fatality. Because of its critical function in processing the polyproteins translated from the positive sense-single stranded RNA virus, the key protease main protease (M^{pro}, also known as $3CL^{pro}$) is an appealing drug target for SARS-CoV-2. Hence, protease inhibitors can play a potential role in inhibiting the functionality of main protease.

In this study, SARS-CoV-2 M^{pro} was used as drug target for identification of potential inhibitors. Virtual screening of 12 PREP inhibitors, and two reference inhibitors were performed against the main protease (PDB ID: 6LU7). The N3 and α-ketoamide 13b compounds were taken as reference inhibitors and were docked against the M^{pro} resulting in a binding affinity of -7.20kcal/mol and -8.52kcal/mol respectively. These references were used to compare the docking scores and molecular interactions of PREP inhibitors with the M^{pro}. Out of the 12 inhibitors, six (KYP-2101, KYP-2091, KYP-2112, S170 92, KYP-2153 and KYP-2108) showed better results. The KYP-2101 showing the best binding score of -9.56kcal/mol and better molecular interactions in comparison to the reference inhibitors. Therefore, the results show that these inhibitors could be potential inhibitors for the crystal structure of SARS-CoV-2 M^{pro}.

2. INTRODUCTION

Severe Acute Respiratory Syndrome coronavirus-2 (SARS-CoV-2) is a type of coronavirus which is responsible in causing the COVID-19 disease [1]. As the name suggested by the WHO, on 31 December 2019, the first case was reported at Wuhan, China [1]. SARS-CoV-2 is a member of *Coronaviridae* family [1]. SARS-Cov and MERS-CoV also belong to the same family. In comparison to other coronaviruses which causes mild infections, these three zootonic viruses belong to the same genus *Betacoronavirus* and are capable of causing serious respiratory infections in humans. SARS-CoV-2 viral vector has a diameter which ranges from 50 to 200 nanometers and ranges from 26 to 32 kilo-base pairs and is accounted as one of the largest known RNA virus [2]. The single-stranded, positive-sense RNA (+ssRNA) includes not less than 6 ORFs. The Open Reading Frames (ORFs) encodes for two NSPs (non-structural proteins), accessory proteins and the remainder of them, structural proteins [2].

According to different studies, SARS-CoV-2 and SARS-CoV both have been found to be 80% similar in sequence identity[3]. Both the types of coronaviruses bind to the ACE (angiotensin-converting enzyme) receptor which has been identified as the functional receptor of the same. Being a zootonic virus, it can cause and transmit from humans to humans. The infection causes mild to severe symptoms in different beings and has higher transmission rates than any other type of coronavirus [4]. Because of this, the whole world has taken a toll and loss of economy and life has taken place to a great extent.

Having no previous encounter with the virus, it is completely new to our immune system. As a result, no pre-existing immunity has been found in our body to fight the viral organism. Common symptoms which is visible in a COVID-19 infected person includes fever, body-aches, temporary impairment in taste and odour and in severe cases, difficulty in breathing [5]. Severe cases may also result to Acute Respiratory Distress Syndrome (ARDS), multiple organ dysfunction, shock and clotting of blood. The incubation period is discovered to be of five days but may span from two to fourteen days [6].

With this being a communicable disease, this virus is primarily spread through small droplets developed by sneezing, talking, and coughing. The droplets less often travel distances of 1 meter

through the air and usually attach to the surface the droplets fall. People may catch the disease by accessing a polluted substance and then eyes and mouth, or by coming in contact with an infected person. It is still possible to spread the disease before the symptom appears or even when a person is asymptomatic i.e. contains no symptoms at all. The popular diagnostic approach is by a nasopharyngeal swab in real-time transcription polymerase chain reaction (RT-PCR). A fast and inaccurate method is the Rapid (Antigen based) test. Based on risk factors and symptoms Chest CT imaging could also be used for evaluation, in people having complex disease symptoms [6].

SARS-Cov-2 Genome Structure

The SARS-CoV-2 genome includes a total number of six ORFs, out of six, two genes are ORF1a and ORF1b (Figure 1). The two large genes encodes for 16 non-structural proteins i.e. NSp1 to NSP16 and contributes about two thirds of the length of the whole genome. ORF 1a and 1b are present at the 5' end respectively, encodes for polyprotein 1a and 1b (pp1a, pp1b) [5]. The 3' end ORF encodes structural proteins known as M, S, E and N. Membrane Proteins (M) brings shape to the viron structure. Envelop proteins (E) is imperative for the maturation and release of the viron particle. In the packing of the RNA genome and virions, the nucleocapsid proteins (N) play an important role as well as having inhibitory role in the disease virulence as an interferon inhibitor (IFN). Apart from the structural proteins, other structural and accessory proteins are unique to animals, such as the HE protein. 3a/b protein and 4a/b proteins are also present beside the four principal structural proteins [7].

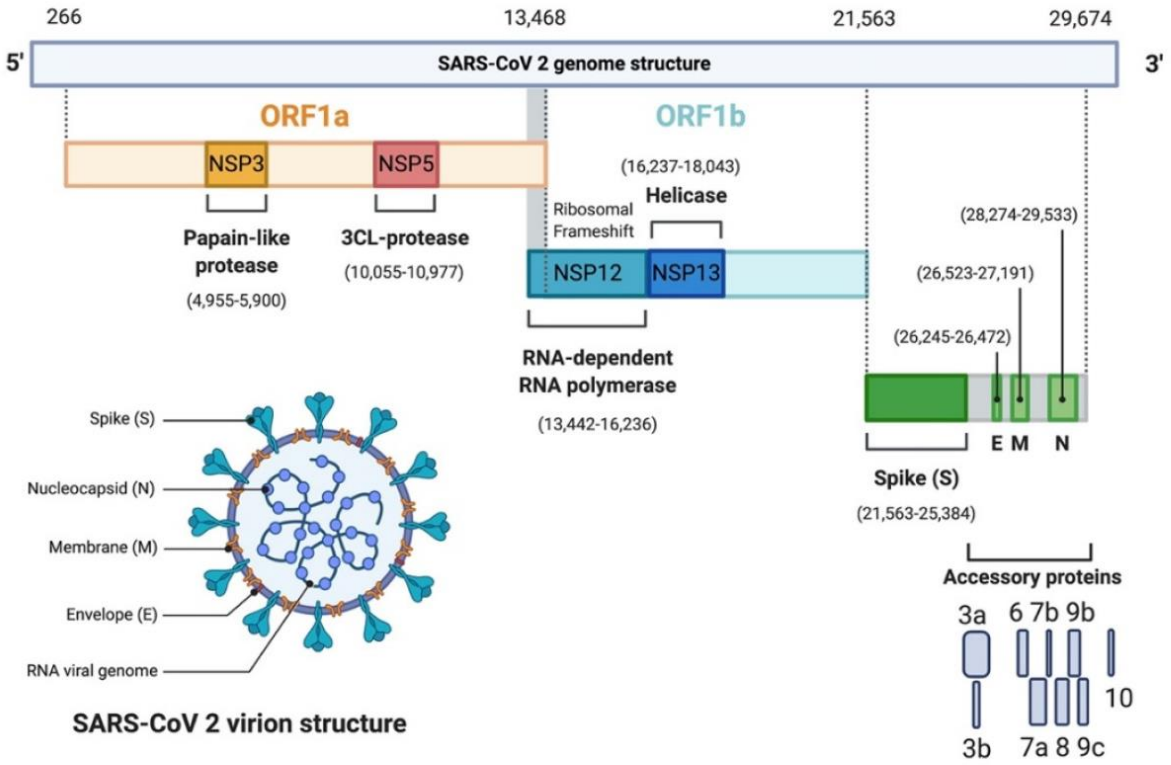

Figure 1. SARS-CoV-2 genome structure**.**

STRUCTURE OF SARS-CoV-2 VIRION

SPIKE PROTEIN (S): The S protein, also called the spike protein has a homotrimeric structure. The crown-like corona appearance is because of the spike protein. There are in total 2 domains present in the S protein, which are the S1 domain, which is the N- terminal domain and the S2 domain that is the C- terminal domain. The S2 domain contains the putative fusion peptide, HR1 (Heptad repeat 1) and HR2 (Heptad repeat 2). Transmembrane domain is also present in S protein [5].

MEMBRANE PROTEIN (M): It is responsible for the shape of the virus and provides structure. The size of M protein is around 25-30KDa and has a dimeric organization.

ENVELOPE PROTEIN (E): It is a small protein of around 8-12KDa in size. The assembly followed by release of the virus is the function of envelope protein.

NUCLEOCAPSID PROTEIN (N): The organization of the RNA genome is done by the nucleocapsid protein. There is a total number of two domains i.e, NDT (N- Terminal Domain) and CTD (C- Terminal Domain).

SARS-CoV-2 Life Cycle

The first step in the ontogenesis of the SARS-CoV-2 is the binding of viron structure to the host cell by the spike protein (Figure 2). S1 subunit of the two units in Spike protein is responsible for the attachment of viron to the host ACE-2 (angiotensin-converting enzyme 2) receptor. The next step, fusion of viron to the membrane of the cell, is followed by the protelytic cleavage of the spike protein into S1 and S2 subunits. These are mediated by cathepsin, some other proteases as well as TMPRSS2 (transmembrane protease serine 2) [2]. TMPRSS2 is responsible for the starting of the plasma membrane and viral membrane fusion. It is less capable to be detected by the antiviral agents in our body and is more beneficial for duplication of the viron.

Translation of polyproteins are followed by release of RNA viron in the host organism. The most important step is then initialized, i.e. the encryption of the NSPs (non-structural proteins). It plays a very important role in RNA viron sythesis and viral congregation [2]. The respective polyproteins, pp1a and pp1ab, are transcribed which are cleaved by the Papain-like protease (Pl^{pro}) and 3C-like protease($3CL^{pro}$). The functional NSPs fabricated are Helicase and the RNA replicase–transcriptase complex (RdRp).

The structural proteins are transcribed by RdRp that are latched to the ER and its surface for viral assembly. The precursor protein along with nucleocaspid protein are dispatched to the ER along the Golgi apparatus to the outer membrane.

The final step is the detachment of the viron structure by a process called exocytosis. These viron then find another host organism for infection and replication.

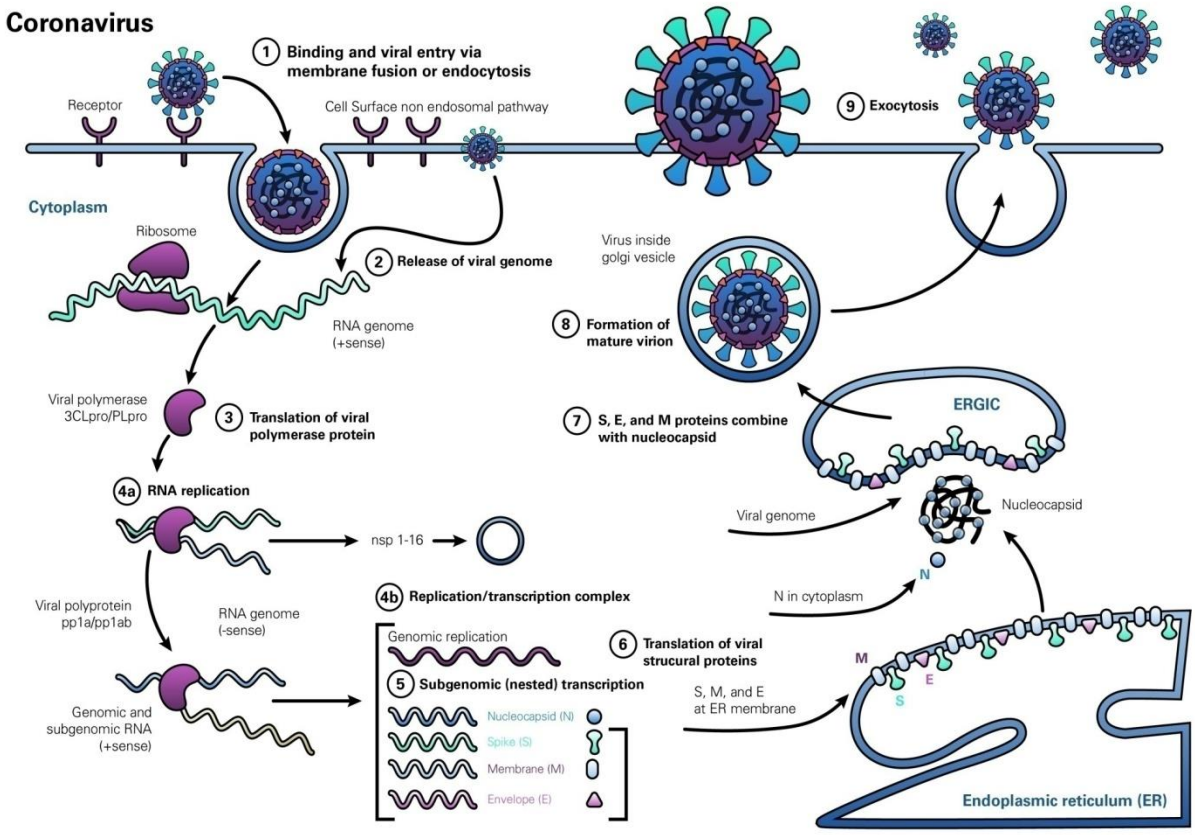

Figure 2. SARS-CoV-2 life cycle.

3. LITERATURE REVIEW

SARS-CoV-2 3CL^{pro}

The SARS-CoV-2 3CL^{pro} also known as the main protease is a proteolytic enzyme which is responsible for breaking down polyproteins at certain sites. Another name for the M^{pro} is C30 endopeptidase or 3CL^{pro}. They are assembled by the polyproteins 1a and 1ab. Both the proteases main protease and papain-like protease (PL^{pro}) are important for the replication of virus, but our area of interest is only the Main Protease. Inhibition of the before mentioned protease is important for viron inactivity because they are responsible for enabling an important step, i.e. cleaving the polyproteins 1a and 1ab to functional proteins. As a result, NSP13 also known as RdRp is unable to work properly without the proteolytic enzyme which is essential for the replication step [8].

The main protease is a thiol proteinase that is responsible for the cleavage at 11 different sites of the viron poplyprotein. It's two identical monomers consists of histidine (HIS) and cysteine (CYS) and also includes the buried water molecule which is considered as the third residue [8].

The SARS-CoV-2 Main protease includes three domains (Figure 3). The first and second domains have amino acids ranging from 81-101 and 102-184, respectively. The third domain has residues from 201-306 and is bridged to the second domain (185-200). The former two domains include anti-parallel β-barrel sheets while the III domain incorporates 5 α-helices. N-terminal finger are present at the residue numbers 1-7 which helps in binding of the promoters. They are located between the domain second and third [8].

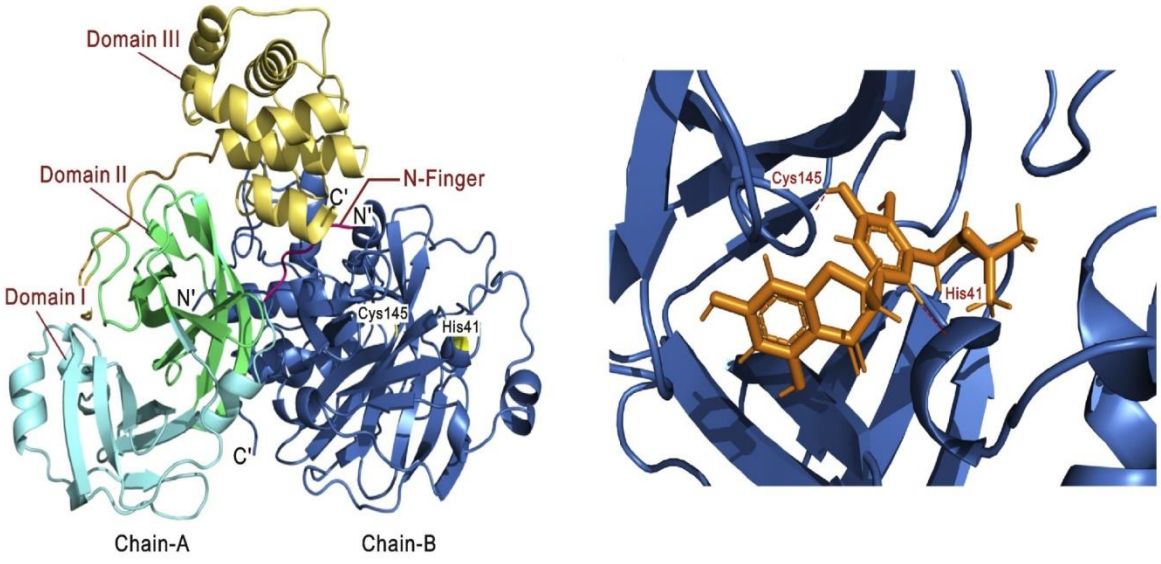

Figure 3. SARS-CoV-2 M^{pro}.

4. MATERIALS AND METHODS

4.1 SELECTION OF TARGET MOLECULES AND REFERENCE INHIBITORS

Target M^{pro} protein structure was downloaded from the RCSB PDB website (https://www.rcsb.org/) with PDB ID: 6LU7 [9]. The protein was then visualized with the help of BIOVIA Discovery Studio (DS) Visualizer (Figure 4).

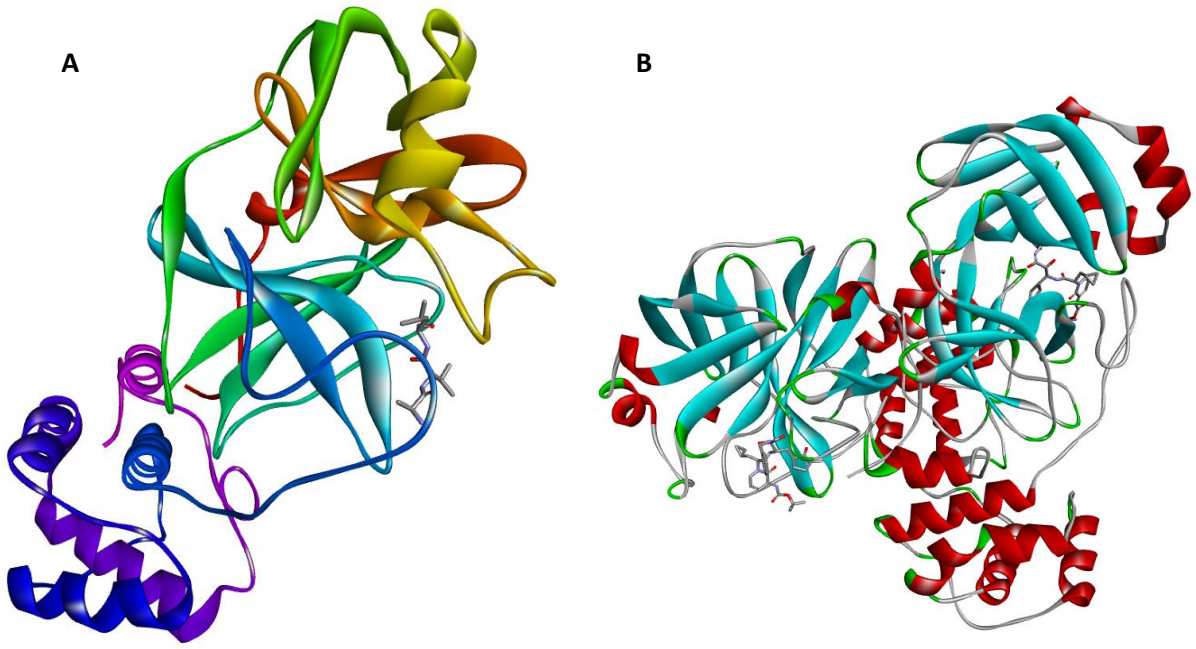

Figure 4. (A) cartoon representation of 6LU7 with N3 inhibitor. (B) cartoon representation of 6Y2G with alpha-ketoamide 13b inhibitor and glycine.

For this study, two reference inhibitors were selected. These are the N-3 and α-ketoamide 13b inhibitors [9, 10]. The N3 inhibitor is found to be effective in blocking the expression of main protease in SARS-CoV and MERS-CoV [6]. It has shown positive results in SARS-CoV-2 M^{pro} as well and has acted as an antiviral agent. The 13b inhibitor, is an alpha ketoaminde inhibitor. The ketoamide have the advantage that their reactive groups can interact with the catalytic center of the target proteases via two hydrogen-bonding interactions as other warheads such as aldehydes or Michael acceptors (N3) can only interact with one (Figure 5).

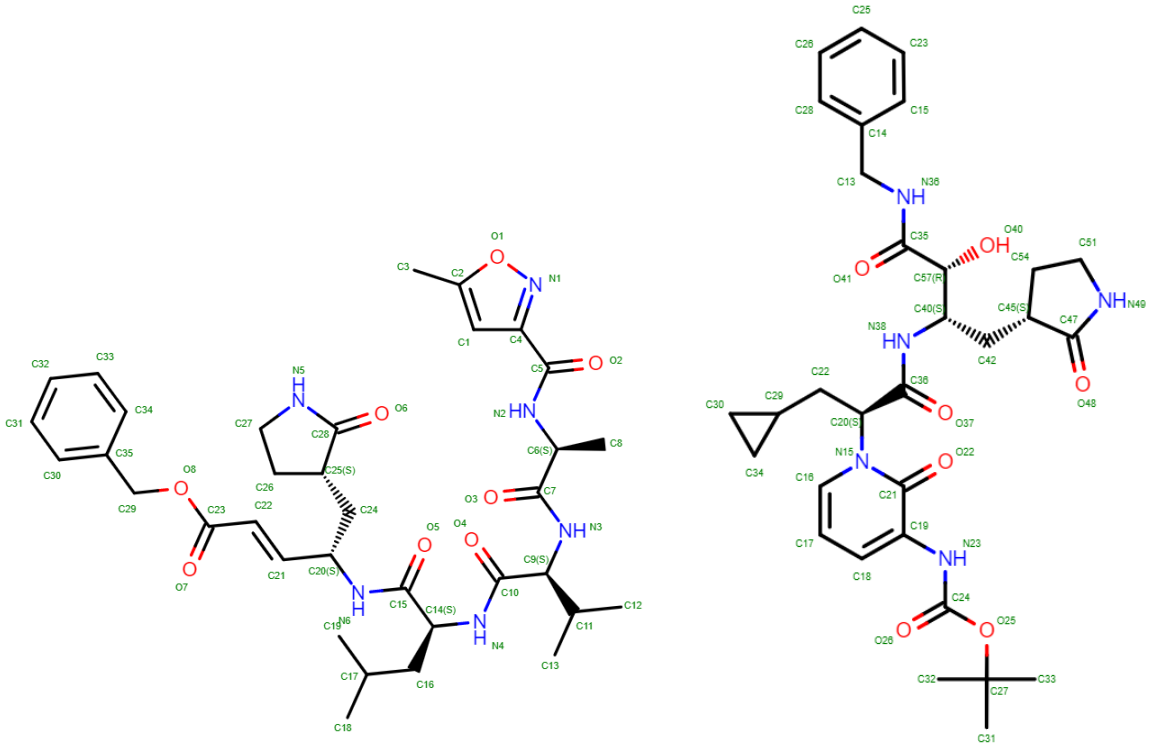

Figure 5. Chemical structure of N3 inhibitor (left), alpha-ketoamide 13b inhibitor (right).

The PDB ID's were prepared by DS. Only one chain was required for our study. The chains, along with ligands were removed from the structure for docking analysis. Heteroataoms were also removed with the help of DS.

4.2 PREPARATION OF MOLECULES

For the docking procedure and analysis, prolyl endopeptidase (PREP) inhibitors were used. Prolyl Oligopeptidase have serine active site which is used for catalysis of endopeptidase. The serine proteases are made up of two domains: α/β hydrolase fold and a β-propeller domain that also is considered to keep larger peptides out from the active site. PREP is expressed in a variety of tissues in both the periphery and the CNS, with the largest amounts occurring in the liver and testis, as well as the prefrontal and nigrostriatal regions of the brain. PREP function has been shown to be altered in brain disorders such as Alzheimer's disorder, Parkinson's disease, Huntington's disease, mania, psychiatric depression, schizophrenia, and autism. PREP inhibitors

have been suggested to treat various neurological disorders [11].In this study, we tried to explore the binding capabilities of PREP inhibitors with SARS-CoV-2 M^{pro}.

We selected 12 tested inhibitors from literature study [11]. The names of the inhibitors are KYP-2047, KYP-2087, KYP-2117, KYP-2101, KYP-2091, KYP-2108, KYP-2112, KYP-2153, KYP-2189, SAUM-1221, S17092 and ZPP (Figure 6). The table was downloaded from the research paper. Out of 12 inhibitors, 8 were in 2D format, so we had to convert each and every compound to 3D. UCSF Chimera was used to convert them to 3D confirmations. KYP-2047, SAUM-1221, S17092 and ZPP were downloaded from ChEMBL database as .SDF format.

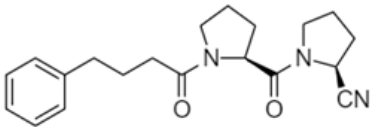

KYP-2047

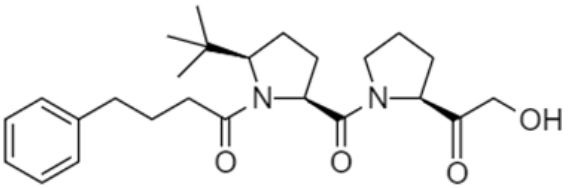

KYP-2117

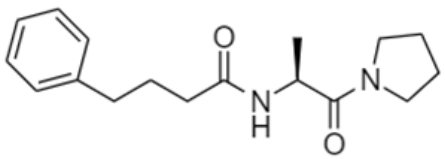

KYP-2087

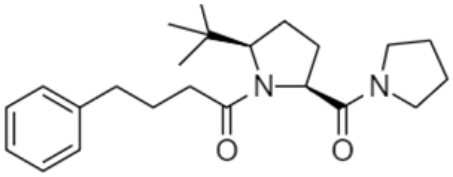

KYP-2101

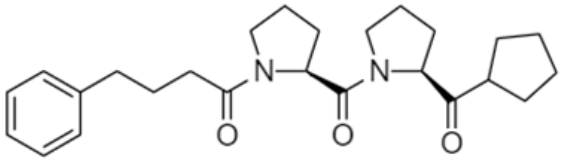

KYP-2091

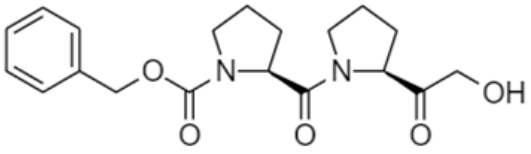

KYP-2108

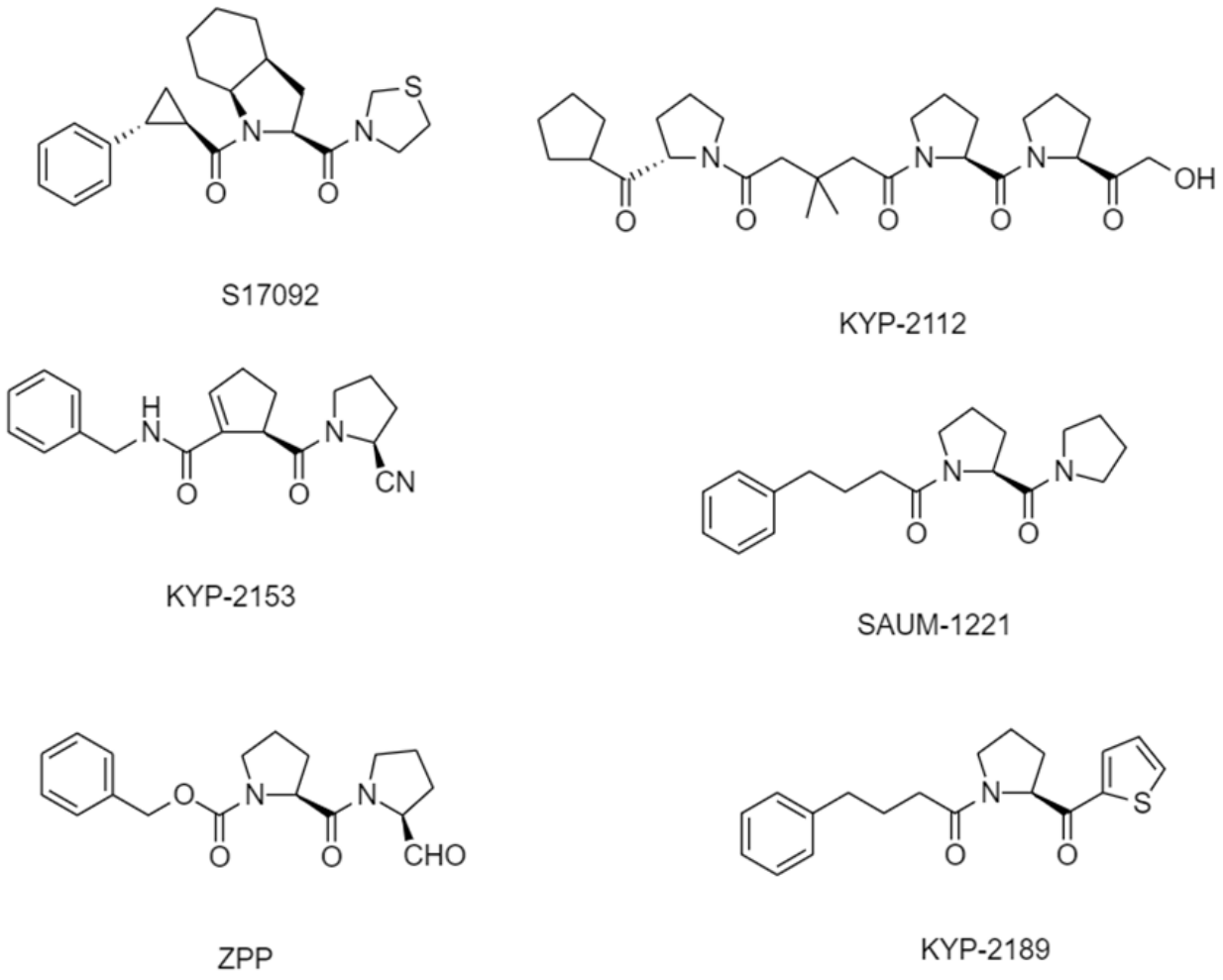

Figure 6. 2D structure of 12 PREP inhibitors.

The converted 3D structures were downloaded in the .mol2 format. Energy minimization step was performed using Chimera 1.14 version. Then, for the docking step the compounds were then converted from .mol2 to .pdbqt by OpenBabel software [12]. The structures which were downloaded from ChEMBL as SDF format was also converted to .pdbqt.

4.3 IDENTIFICATION OF BINDING SITE

The inhibitor binding site was determined within 5Å of the cocrystal of downloaded M^{pro} structure. The visual representation is shown below (Figure 7).

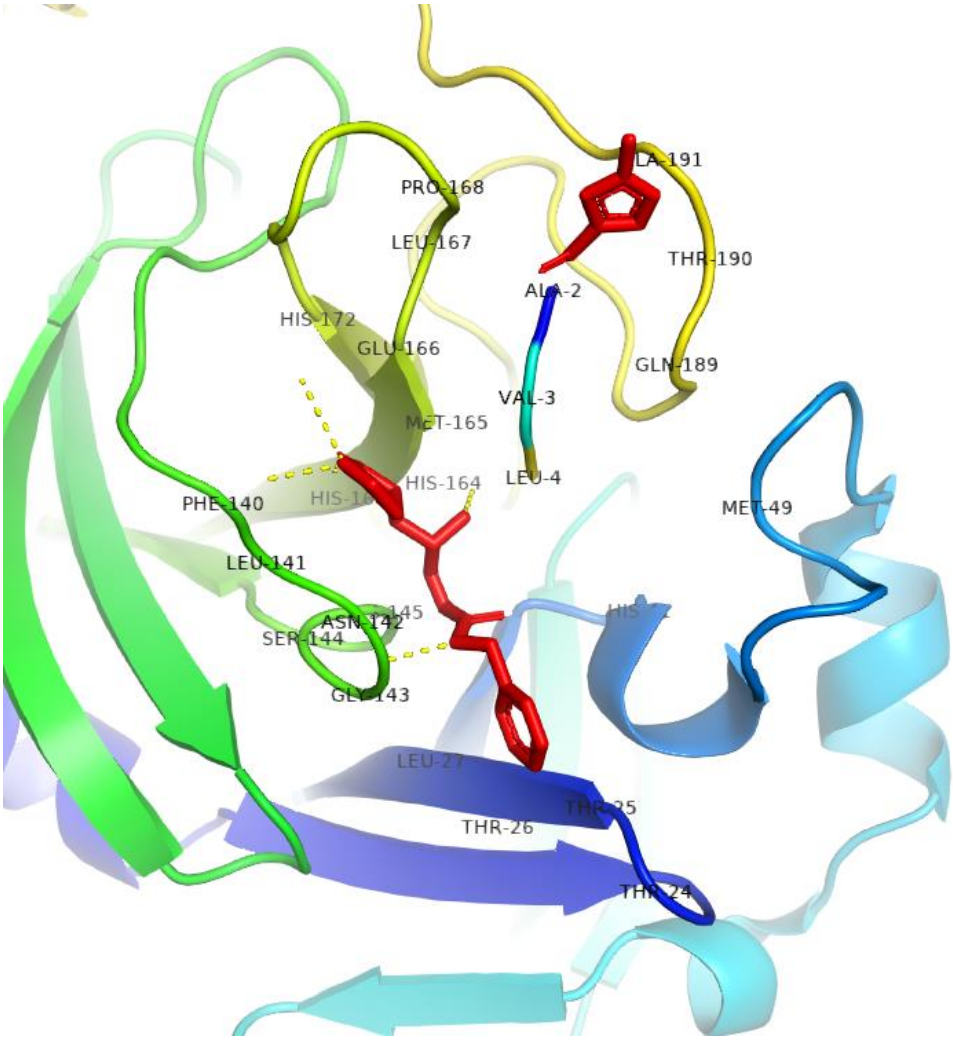

Figure 7. Binding site visualization.

For the identification of the active sites, where the ligands will bind to the receptor, PyMol Visualization software was used. The process for the active site identification was same for both the PDB crystal structures. After uploading the crystal structure of the SARS-CoV-2 main protease in PyMOL, the first step is to remove water molecules. Select preset in actions, and then followed by ligands to make the view more clear. The protein backbone can also be kept hidden.

the active site residues of 6LU7 (Table 1) includes MET49, GLN189, THR190, ALA191, MET165, GLU166, LEU167, PRO168, HIS172, HIS41, THR25, THR26, LEU27, CYS145, GLY143, HIS164, HIS163, LEU141, ASN142, SER144, PHE140, THR24.

The table of the active sites residues for 6LU7 are also shown below:

Table 1. Active site residues forming the binding cavity.

S.NO	AMINO-ACID POSITION	S.NO	AMINO ACID POSITION
1	MET49	12	THR26
2	GLN189	13	LEU27
3	THR190	14	CYS145
4	ALA191	15	GLY143
5	MET165	16	HIS164
6	GLU166	17	HIS163
7	LEU167	18	LEU141
8	PRO168	19	ASN142
9	HIS172	20	SER144
10	HIS41	21	PHE140
11	THR25	22	THR24

4.4 PREDOCKING STUDY

The reference inhibitor (N3) was re-docked with the help of Autodock 4. This is a critical step before conducting virtual screening. The coordinates for the co-crystal ligand were taken from the respective PDB structure (6LU7). Molecular docking was performed for N3 against the SARS-CoV-2 M^{pro}.

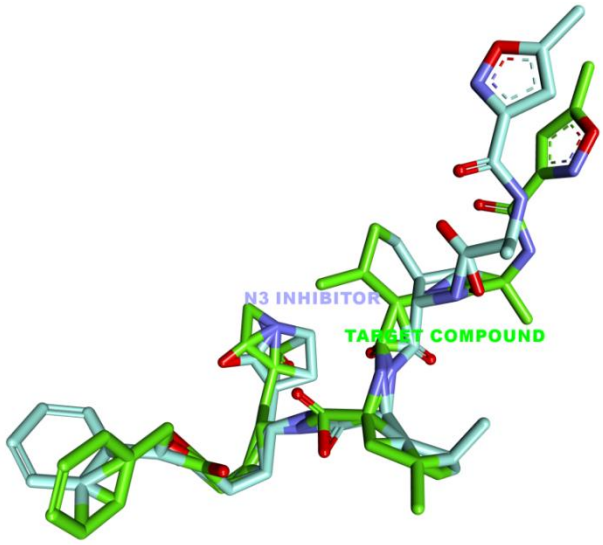

Figure 8. Superimposition of docked pose (blue) of co-crystal ligand over crystal conformation (green).

The docked poses were then compared with the target compound with the help of an online tool i.e. LS-align [13]. The tool uses enhanced-greedy based, iterative heuristic search algorithm. The flexible align parameter resulted in an acceptable RMSD (Root Mean Square Deviation) value of 1.96 Å (Figure 8). Docking results shows us that N3 binds to SARS-CoV-2 M^{pro} with an binding energy of -7.20 kcal/mol.

4.5 MOLECULAR DOCKING

The reference inhibitors N3 and 13b were docked with the help of Autodock 4 of Autodock Tools-1.5.6 against SARS-CoV-2 M^{pro} (6LU7). The pdbqt files of the respective inhibitors were uploaded. Unwanted ligands and chains were removed along with hydrogen atoms. Polar hydrogens and Gasteiger chargers were also added (-3.0035). The residues described above were selected (Table 1). The grid parameters had coordinates of x:86, y:78 z:78 and x_center: -15.492, y_center: 13.998, z_center: 66.638.

The Autodock uses a generic algorithm for docking calculations. The number of GA runs were set to 100 for redocking, and 10 for PREP inhibitors respectively. The docking result is saved in dock.dlg file which includes the Binding affinities and the coordinates for the docked poses. The ligand-receptor interaction was studied with the help of DS software.

5. RESULTS AND DISCUSSION

The crystal structure of SARS-CoV-2 M^{pro} was used to screen PREP inhibitors. The docking study consisted of a total number of 12 PREP inhibitors. The results presented in Table 2 shows the binding energies (kcal/mol) of both the reference inhibitors as well as 12 compounds. The binding energies are present in descending order with the reference inhibitors marked in bold. The protein ligand interactions are also visible in the table below (Table 2).

Table 2. Binding energy of reference and target inhibitors along with interaction with the protein. The reference inhibitors are shown in bold.

S.NO	COMPOUNDS	BINDING ENERGY	HYDROGEN BOND INTERACTIONS
1	KYP-2101	-9.56	GLU-166
2	KYP-2091	-9.46	GLU-166,GLN-189
3	KYP-2112	-9.01	CYS-145, GLY-143, SER-144, THR-26
4	S17092	-8.88	GLU-166, ARG-188
5	KYP-2153	-8.66	GLU-166, ARG-188
6	KYP-2108	-8.58	GLN-192, THR-190
7	**13b**	**-8.52**	**GLU-166**
8	KYP-2189	-8.12	GLY-143
9	KYP-2047	-6.95	CYS-145, GLY-143, SER-144
10	KYP-2087	-7.91	GLU-166,GLN-189
11	KYP-2117	-7.82	MET-49, TYR-54
12	SUAM-1221	-7.70	GLU-166
13	**N3**	**-7.20**	**CYS-145, GLY-143, GLU-166, ASN-142, LEU-141, GLN-189**
14	ZPP	-7.40	GLU-166

Below are the respective inhibitors and its interaction with the target protein i.e. 6LU7. The various interactions include van der waals interaction which is light blue in color. π-π alkyl interactions in pink color and Hydrophobic interactions which is in green colour. Other interactions such as π-sulphur are denoted with yellow colour.

Out of the total number of 12 inhibitors, six have shown better results i.e. KYP-2101, KYP-2091, KYP-2112, S17092, KYP-2153 and KYP-2108. The reference inhibitor N3 has binding energy of -7.20 kcal/mol (Table 2). Molecular interactions have also been shown (Figure 9) having amino acids, CYS-145, GLY-143, GLU-166, ASN-142, LEU-141, GLN-189 interacting with the N3 inhibitor. Binding energy of α-ketoamidase 13b has come out to be -8.52 kcal/mol (Table 2). GLU-166 is found to be interacting with the ligand as conventional hydrogen bonding (Figure 10).

KYP-2101 is the best scoring compound in our study. Binding energy of the compound is -9.56 kcal/mol (Table 2). GLU-166 is the hydrogen bond interaction (Figure 11) which is common amino acid to the reference inhibitor 13b. CYS-145, HIS-41, MET-165 and PRO-168 form the π-π alkyl interactions. KYP-2091 is the second best scoring compound in our study. Binding energy of the compound is -9.46 kcal/mol (Table 2). GLU-166 and GLN-189 are the hydrogen bond interactions (Figure 12), which are also common amino acids to the reference inhibitor 13b and N3. HIS-163, MET-165 and PRO-168 form the π-π alkyl interactions. KYP-2112 is the third best scoring compound in our study. Binding energy of the compound is -9.01 kcal/mol (Table 2). CYS-145, GLY-143, SER-144, THR-26 are the hydrogen bond interactions (Figure 13), where CYS-145 and GLY-143 are found to be common amino acids to the reference inhibitor N3. LEU-27, HIS-41, MET-49 and MET-165 form the π-π alkyl interactions. S17092 is the fourth best scoring compound in our study. Binding energy of the compound is -8.88 kcal/mol (Table 2). GLU-166 and ARG-188 are the hydrogen bond interaction (Figure 14) which is common to the reference inhibitor N3 and 13b. PRO-168, HIS-41, MET-165 form the π-π alkyl interactions. KYP-2153 is the fifth best scoring compound in our study. Binding energy of the compound is -8.66 kcal/mol (Table 2). GLU-166 and ARG-188 are the hydrogen bond interactions (Figure 15) which is common to the reference inhibitor N3 and 13b. PRO-168, HIS-41, MET-165 form the π-π alkyl interactions. KYP-2108 is the sixth best scoring compound in our study. Binding energy of the compound is -8.58 kcal/mol (Table 2). GLN-192 and THR-190 are having the hydrogen bond interactions (Figure 16). PRO-168, HIS-163, MET-165 and CYS-145 form the π-π alkyl interactions. Rest of the compounds, KYP-2189 (Figure 17), KYP-2047 (Figure 18), KYP-2087 (Figure 19), KYP-2117 (Figure 20), SUAM-1221 (Figure 21) and ZPP (Figure 22) have also been represented in 3D as well as 2D confirmations respectively.

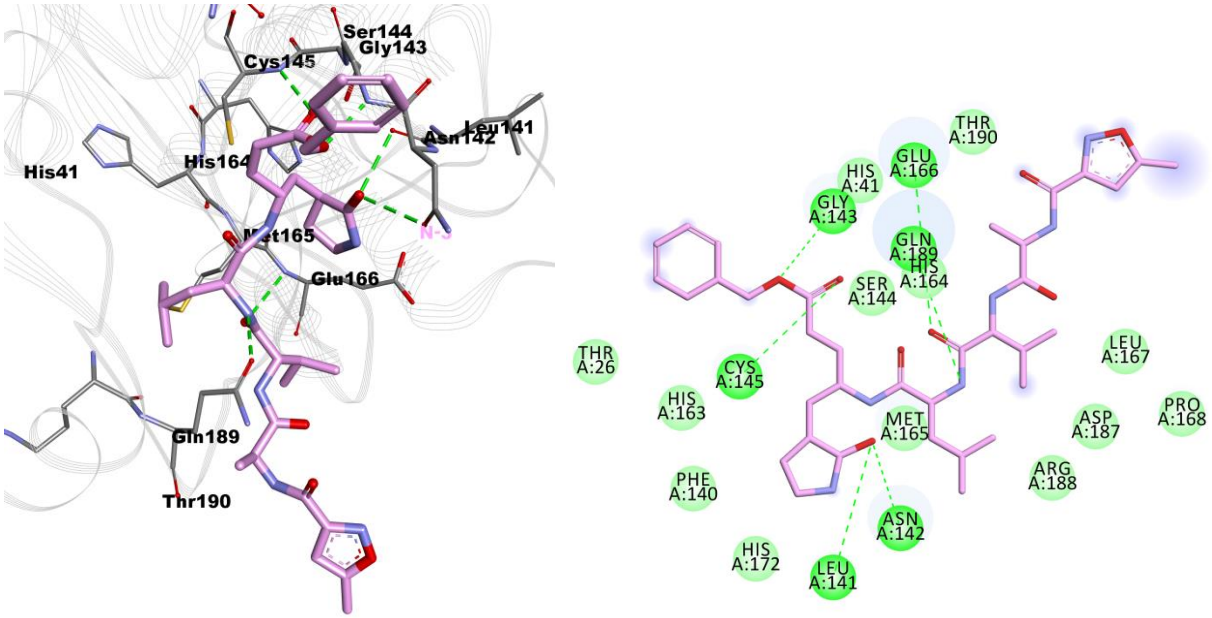

Figure 9. 3D (left) and 2D (right) representation of N3 with its interactions.

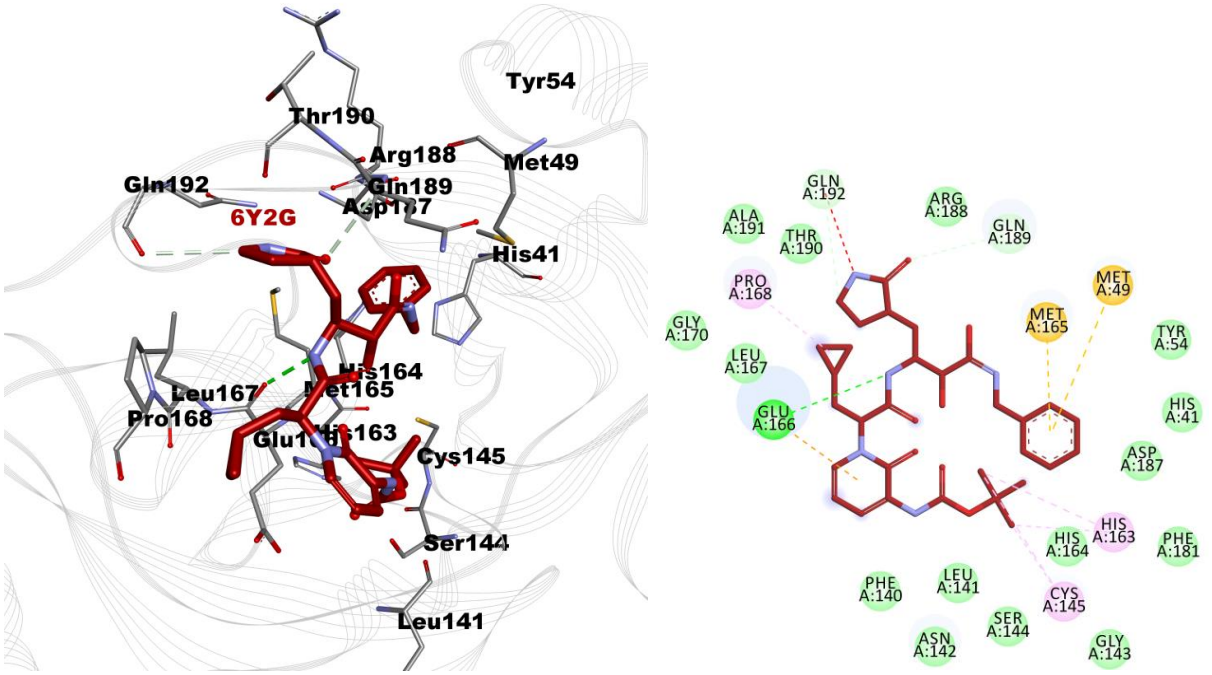

Figure 10. 3D (left) and 2D (right) representation of α-ketoamide 13b with its interactions.

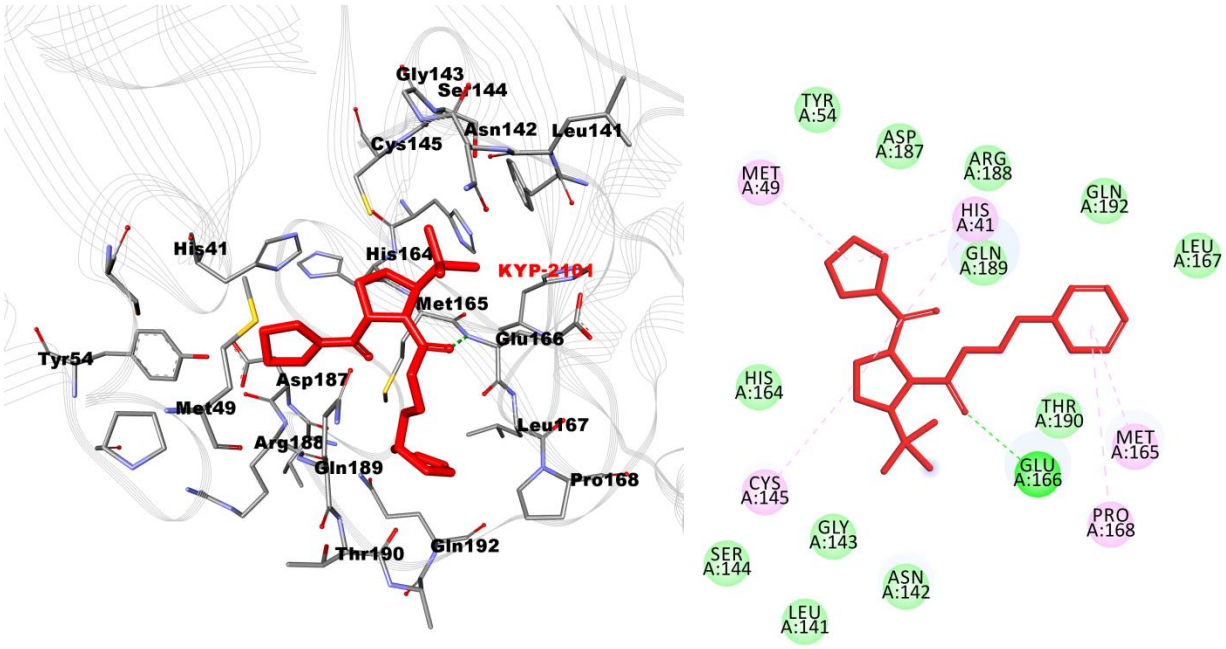

Figure 11. 3D (left) and 2D (right) representation of KYP-2101 with its interactions.

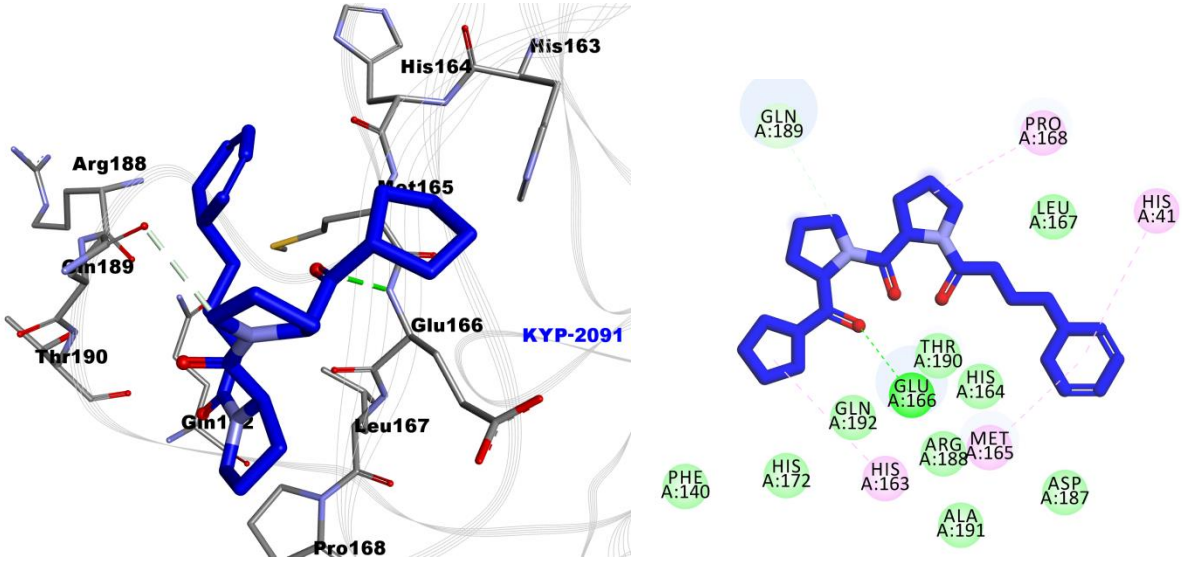

Figure 12. 3D (left) and 2D (right) representation of KYP-2091 with its interactions.

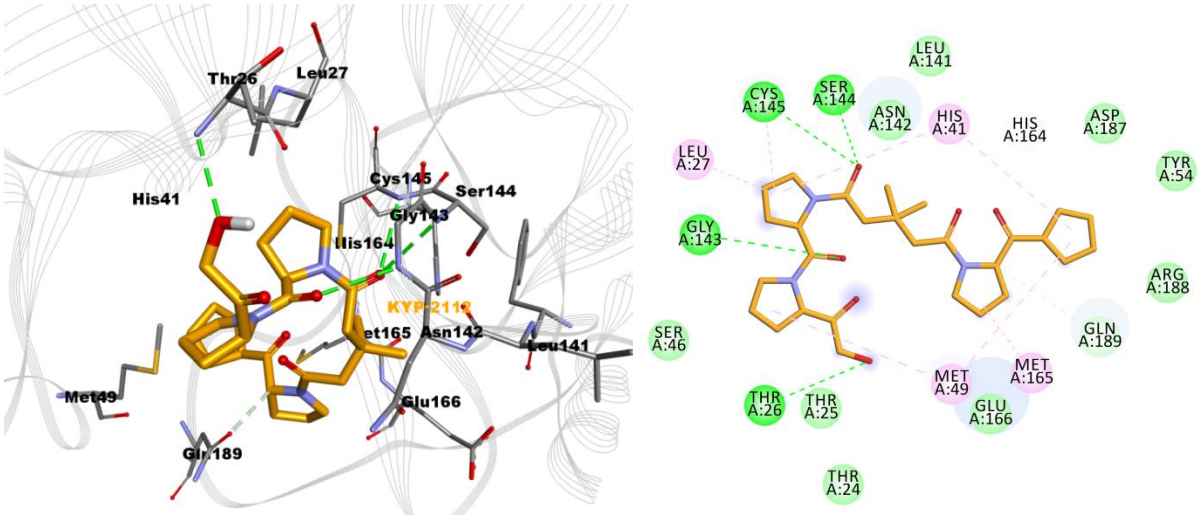

Figure 13. 3D (left) and 2D (right) representation of KYP-2112 with its interactions.

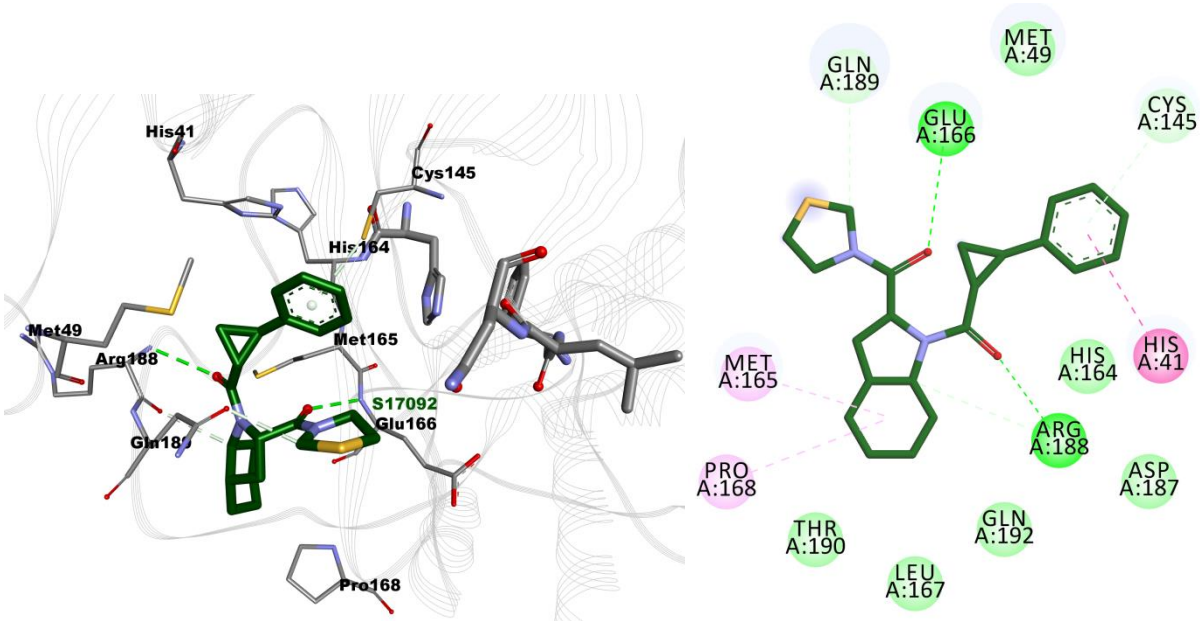

Figure 14. 3D (left) and 2D (right) representation of S17092 with its interactions.

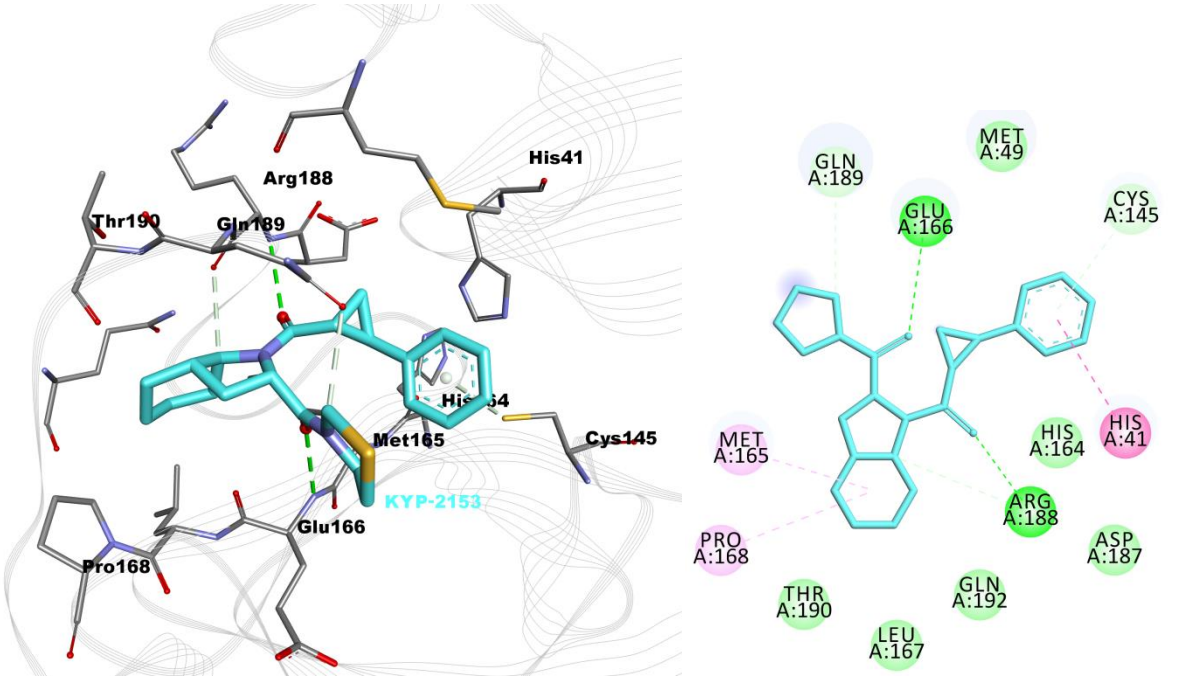

Figure 15. 3D (left) and 2D (right) representation of KYP-2153 with its interactions.

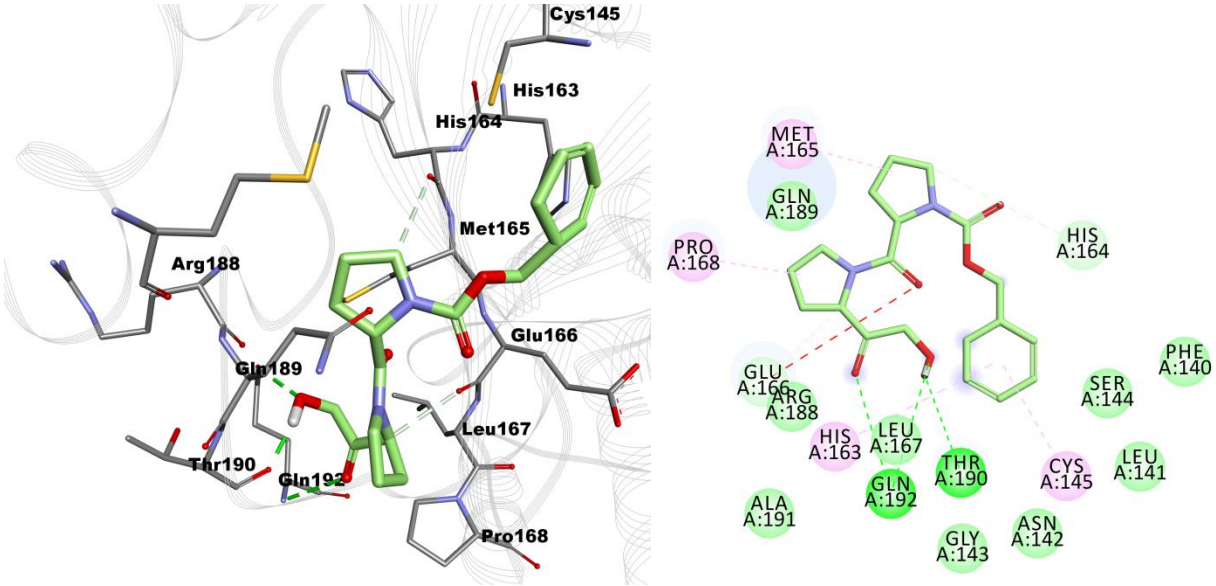

Figure 16. 3D (left) and 2D (right) representation of KYP-2108 with its interactions.

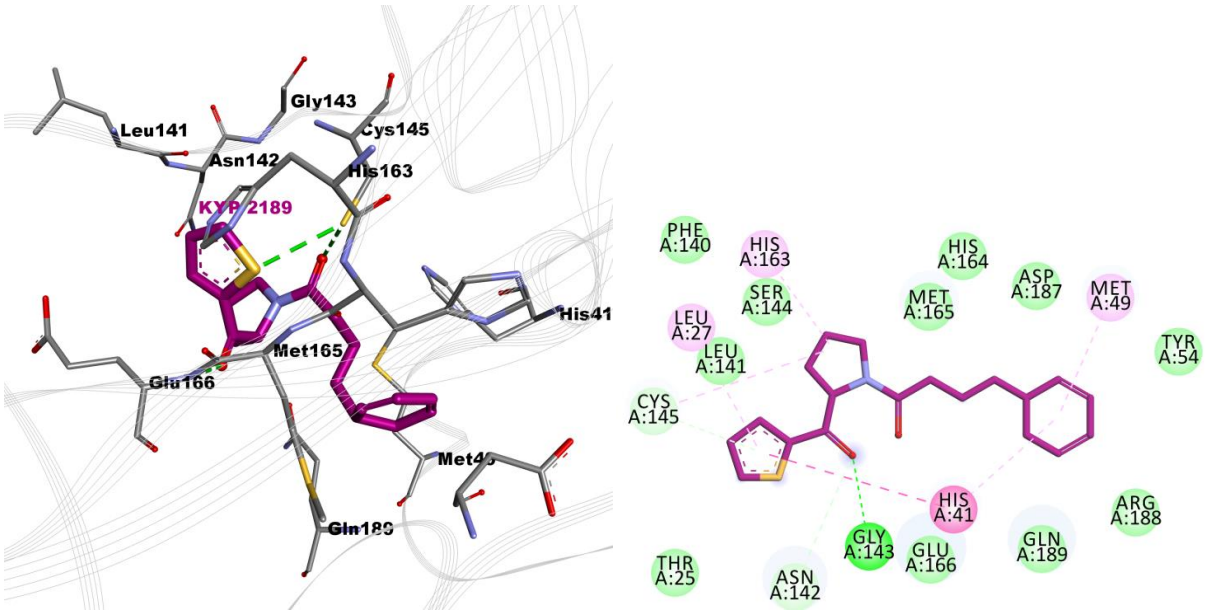

Figure 17. 3D (left) and 2D (right) representation of KYP-2189 with its interactions.

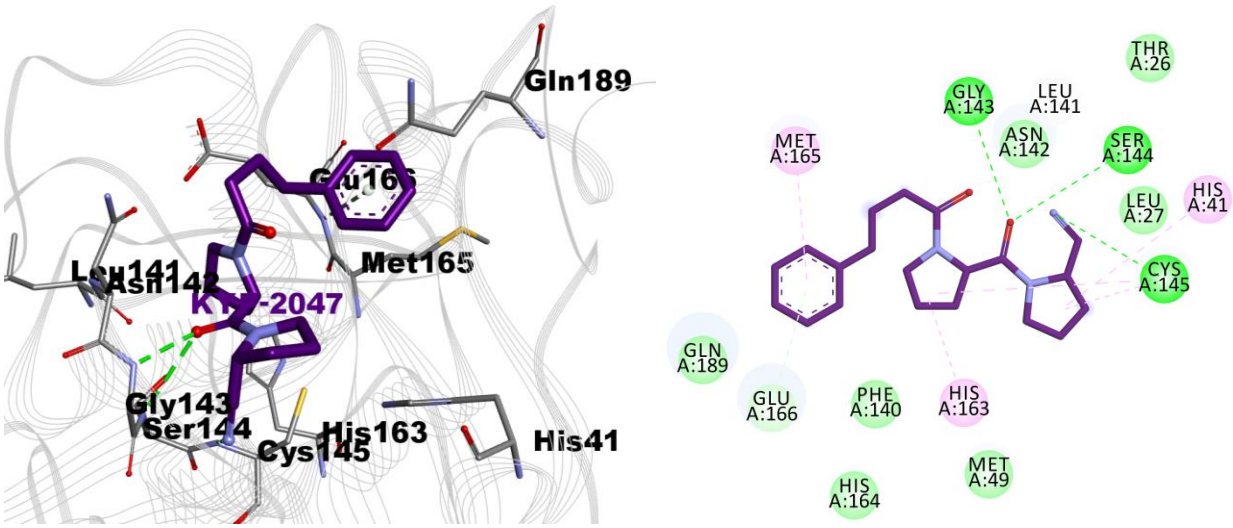

Figure 18. 3D (left) and 2D (right) representation of KYP-2047 with its interactions.

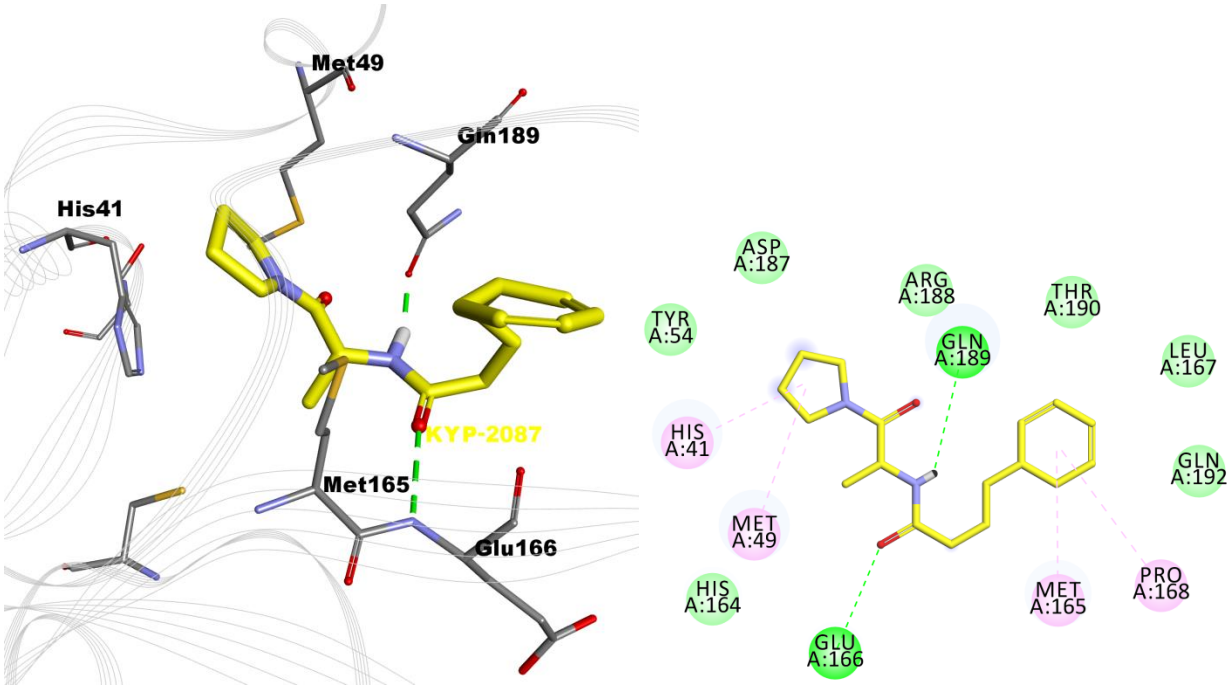

Figure 19. 3D (left) and 2D (right) representation of KYP-2087 with its interactions.

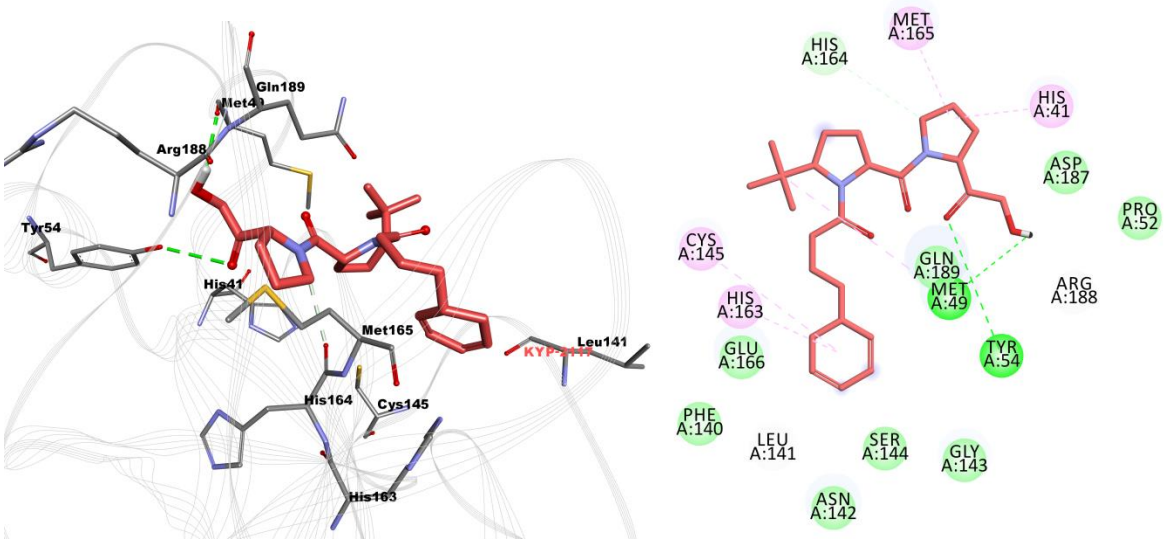

Figure 20. 3D (left) and 2D (right) representation of KYP-2117 with its interactions.

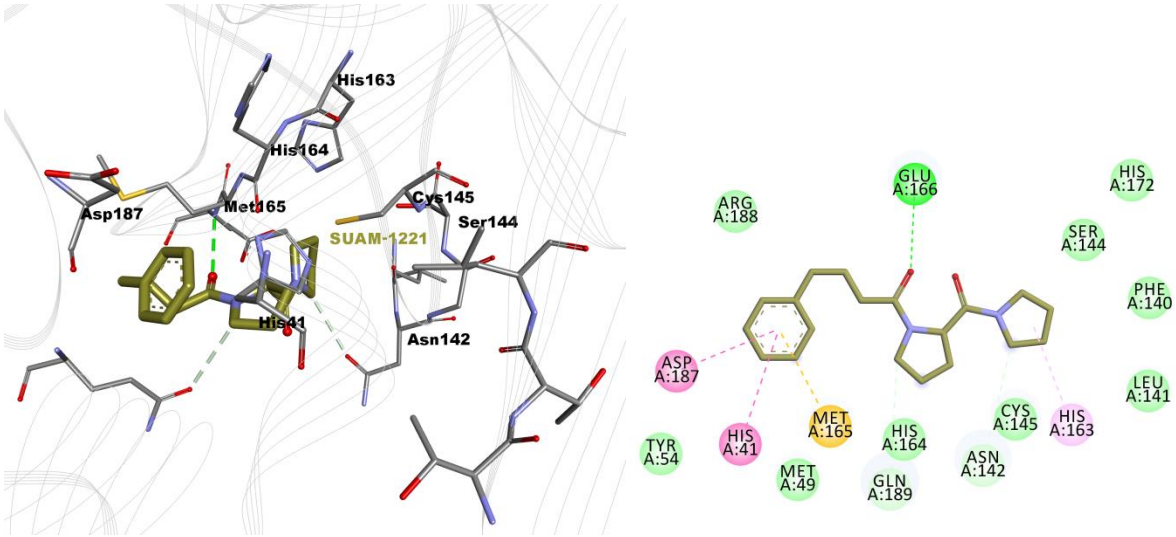

Figure 21. 3D (left) and 2D (right) representation of SUAM-1221 with its interactions.

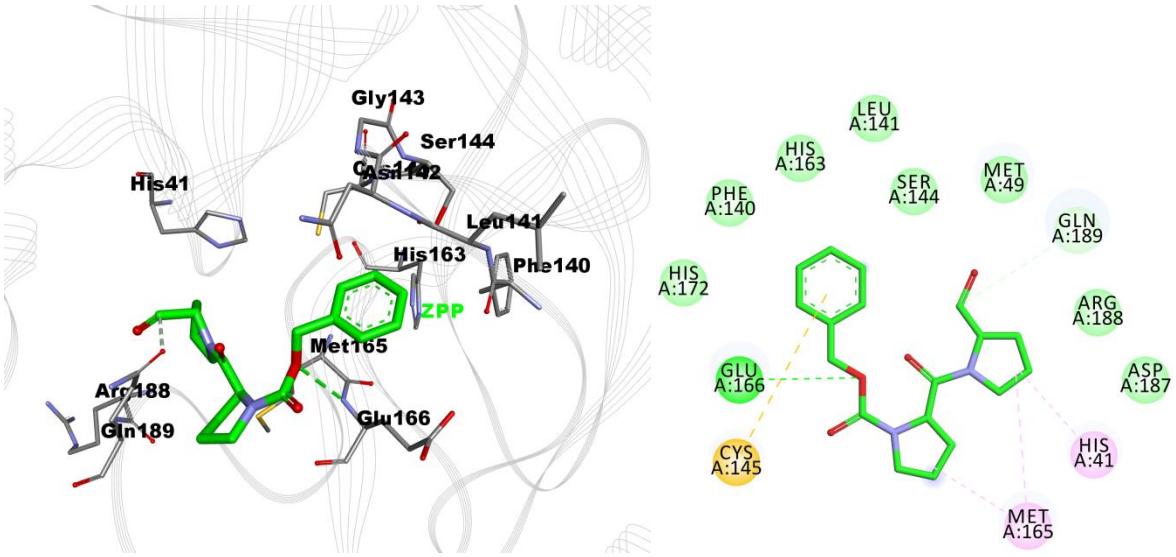

Figure 22. 3D (left) and 2D (right) representation of ZPP with its interactions

6. CONCLUSION

The COVID-19 pandemic is indeed a huge menace to humanity. Given the gravity of the ongoing crisis, various efforts to improve vaccines and antiviral drugs are underway. Because of the magnitude of the COVID-19 pandemic, the only way to identify a timely successful cure is to repurpose certified medications. Many vaccines and drugs are already been discovered and tested positive results on patients. In terms of drug production, the main protease of SARS-CoV-2 reaches out with a potential viral candidate due to major differences from human proteases. We screened a library of 12 PREP inhibitors using a combination of virtual screening and molecular docking techniques. The above mentioned PREP inhibitors (KYP-2101, KYP-2091, KYP-2112, S17092, KYP-2153 and KYP-2108) presented with better results as compared to the reference inhibitors, with KYP-2101 showing the best score. The six inhibitors provided better binding affinities and molecular interactions thus, would be presumably efficient in inhibition of the SARS-CoV-2 main protease.

7. REFERENCES

[1] T. Singhal, "A Review of Coronavirus Disease-2019 (COVID-19)," *Indian J Pediatr*, vol. 87, no. 4, pp. 281–286, Apr. 2020

[2] C. Gil *et al.*, "COVID-19: Drug Targets and Potential Treatments," *J. Med. Chem.*, vol. 63, no. 21, pp. 12359–12386, Nov. 2020

[3] M. Tahir ul Qamar, S. M. Alqahtani, M. A. Alamri, and L.-L. Chen, "Structural basis of SARS-CoV-2 3CLpro and anti-COVID-19 drug discovery from medicinal plants," *Journal of Pharmaceutical Analysis*, vol. 10, no. 4, pp. 313–319, Aug. 2020

[4] L. Mousavizadeh and S. Ghasemi, "Genotype and phenotype of COVID-19: Their roles in pathogenesis," *Journal of Microbiology, Immunology and Infection*, p. S1684118220300827, Mar. 2020

[5] L. Alanagreh, F. Alzoughool, and M. Atoum, "The Human Coronavirus Disease COVID-19: Its Origin, Characteristics, and Insights into Potential Drugs and Its Mechanisms," *Pathogens*, vol. 9, no. 5, p. 331, Apr. 2020

[6] G. Burmer, M. Burmer, and V. Pabuwal, "SARS-CoV-2 and COVID-19 Pathogenesis: A Review," p. 34.

[7] R. Ahsan, M. R. Tahsili, F. Ebrahimi, E. Ebrahimie, and M. Ebrahimi, "Image processing unravels the evolutionary pattern of SARS-CoV-2 against SARS and MERS through position-based pattern recognition," *Computers in Biology and Medicine*, vol. 134, p. 104471, Jul. 2021

[8] M. Tahir ul Qamar, S. M. Alqahtani, M. A. Alamri, and L.-L. Chen, "Structural basis of SARS-CoV-2 3CLpro and anti-COVID-19 drug discovery from medicinal plants," *Journal of Pharmaceutical Analysis*, vol. 10, no. 4, pp. 313–319, Aug. 2020

[9] Z. Jin *et al.*, "Structure of Mpro from SARS-CoV-2 and discovery of its inhibitors," *Nature*, vol. 582, no. 7811, pp. 289–293, Jun. 2020

[10] Zhang L;Lin D;Sun X;Curth U;Drosten C;Sauerhering L;Becker S;Rox K;Hilgenfeld R; "Crystal structure of SARS-CoV-2 main protease provides a basis for design of improved α-ketoamide inhibitors," *Science* , May. 2021

[11] T. P. Kilpeläinen *et al.*, "The effect of prolyl oligopeptidase inhibitors on alpha-synuclein aggregation and autophagy cannot be predicted by their inhibitory efficacy," *Biomedicine & Pharmacotherapy*, vol. 128, p. 110253, Aug. 2020

[12] N. M. O'Boyle, M. Banck, C. A. James, C. Morley, T. Vandermeersch, and G. R. Hutchison, "Open Babel: An open chemical toolbox," *J Cheminform*, vol. 3, no. 1, p. 33, Dec. 2011

[13] J. Hu, Z. Liu, D.-J. Yu, and Y. Zhang, "LS-align: an atom-level, flexible ligand structural alignment algorithm for high-throughput virtual screening," *Bioinformatics*, vol. 34, no. 13, pp. 2209–2218, Jul. 2018